



HAL
open science

A modular click ligand-directed approach to label endogenous dopamine D1 receptors in live cells

Xavier Gómez-Santacana, Marin Boutonnet, Carles Martínez-Juvés, Marta Cimadevila, Juanlo Catena, Enora Moutin, Thomas Roux, Eric Trinquet, Laurent Lamarque, Julie Perroy, et al.

► To cite this version:

Xavier Gómez-Santacana, Marin Boutonnet, Carles Martínez-Juvés, Marta Cimadevila, Juanlo Catena, et al.. A modular click ligand-directed approach to label endogenous dopamine D1 receptors in live cells. *Communications Chemistry*, 2025, 8 (1), pp.113. <10.1038/s42004-025-01504-3>. <hal-05047394>

HAL Id: hal-05047394

<https://hal.science/hal-05047394v1>

Submitted on 25 Apr 2025

HAL is a multi-disciplinary open access archive for the deposit and dissemination of scientific research documents, whether they are published or not. The documents may come from teaching and research institutions in France or abroad, or from public or private research centers.

L'archive ouverte pluridisciplinaire HAL, est destinée au dépôt et à la diffusion de documents scientifiques de niveau recherche, publiés ou non, émanant des établissements d'enseignement et de recherche français ou étrangers, des laboratoires publics ou privés.



Distributed under a Creative Commons CC BY-NC-ND 4.0 - Attribution - Non-commercial use - No Derivative Works - International License

<https://doi.org/10.1038/s42004-025-01504-3>

A modular click ligand-directed approach to label endogenous dopamine D₁ receptors in live cells



Xavier Gómez-Santacana^{1,2}✉, Marin Boutonnet¹, Carles Martínez-Juvés², Marta Cimadevila¹, Juanlo Catena², Enora Moutin¹, Thomas Roux³, Eric Trinquet³, Laurent Lamarque³, Julie Perroy¹, Laurent Prézeau¹, Jurriaan M. Zwier^{3,4}, Jean-Philippe Pin¹✉ & Amadeu Llebaria²✉

Most luminescence-based technologies to determine the pharmacological properties of G Protein-Coupled Receptors (GPCRs) rely on the overexpression of genetically modified receptors. However, it is essential to develop approaches allowing the specific labelling of native receptors. Here we report an innovative approach based on the use of molecular modules to build fluorescent ligand-directed probes that can label aminergic GPCRs. Such probes are readily prepared with a click reaction between a ligand that may include nucleophilic groups and a fluorescent electrophilic linker. The rapidity of click reaction before receptor labelling prevents a side reaction between the nucleophilic ligand and the electrophile. This approach allowed us to label D₁ receptor in transfected cells and native receptors in neural cell lines, leaving the receptor fully functional. This approach will pave the way to develop new reagents and assays with which to monitor endogenous GPCRs' distribution, trafficking, activity or binding properties in their native environment.

G protein-coupled receptors (GPCR) are a complex superfamily of membrane proteins that have a key role in regulating many physiological processes, being the target of around 35% of approved drugs¹. Due to their biological relevance, there is a high interest in unveiling signal transduction and developing new compound tools that could be ultimately used in classical medicine as well as innovative theragnostic fields.

In the last two decades, new technologies based on luminescence have been developed to monitor the organisation, trafficking, signalling or ligand binding of GPCRs. These technologies rely on the overexpression of genetically modified receptors and include popular assay technologies such as Bioluminescence and Förster Resonance Energy Transfer (i.e. BRET² and FRET³). A successful example is the Tag Lite[®] technology, developed by Cisbio Bioassays (now Revvity), which is based on genetically modified receptors fused to a suicide enzyme tag, such as the SNAP-tag[®] (ST)⁴. These tagged receptors can be covalently labelled with any type of fluorophore, including lanthanide cryptates (such as Lumi4-Tb⁵) that allow time-resolved fluorescence or TR-FRET measurements with a second fluorophore (i.e. TR-FRET acceptor)⁵. Depending on the nature of the TR-FRET acceptor, this technology can be used in internalisation, oligomerisation or binding assays^{6,7}. For example, the combination of SNAP-tagged receptors

with Lumi4Tb and fluorescent ligands allows final point binding assays (e.g. saturation or competition) or kinetic binding assays (e.g. association, dissociation or association-competition)⁸.

As previously mentioned, these approaches rely on the use of artificial systems, involving overexpression of genetically manipulated proteins in heterologous cells. However, the properties of these modified receptors are unlikely similar to those of the native receptor in its natural environment. Moreover, the labelling of native receptors may be useful for analysing human samples in clinical studies. Therefore, an attractive objective in chemical biology is to extend the high performance assays and protein labelling selectivity of technologies based on genetically-encoded tags to unmodified receptors in their native environments such as within primary cell cultures or tissues^{4,9}.

A critical challenge of such an approach is in the selection of a suitable chemical reaction to specifically label certain amino acid residues of a native protein of interest. Several approaches have been reported to date but the low reactivity and broad abundance of certain amino acid residues add difficulties to the specificity of the conjugation reaction¹⁰. This difficulty grows as the complexity of the system increases: from isolated proteins to cell cultures, tissues or even organisms. Ligand-directed (LD) approaches,

¹Institut de Génomique Fonctionnelle, Université de Montpellier, CNRS and INSERM, Montpellier, France. ²Medicinal Chemistry & Synthesis, Institute for Advanced Chemistry of Catalonia (IQAC), Spanish Council for Scientific Research (CSIC), Barcelona, Spain. ³Revvity, Codolet, France. ⁴Present address: Department of Cognitive Neuroscience, Radboud University Medical Centre, Nijmegen, The Netherlands. ✉e-mail: xavier.gomez@iqac.csic.es; jean-philippe.pin@igf.cnrs.fr; amadeu.llebaria@iqac.csic.es

extensively developed in Hamachi's lab¹¹, may offer a solution to this problem, as recently been proven successful *in vivo*¹². Within a single molecule, an affinity unit for a protein of interest (based on a ligand), a fluorescent label and a reactive moiety (i.e. electrophilic group) are combined, with a relative geometry and distance that, upon ligand binding, directs the labelling reaction to an amino acid in the vicinity of a binding pocket. These reactive moieties include tosylates to conjugate mainly cysteines¹³ or acyl imidazole, dibromophenyl benzoates or *N*-acyl-*N*-alkyl sulphonamides for lysine labelling^{14–17}. Some ligand-directed approaches have been reported to label GPCR for bradykinin B₂¹⁴, Adenosine A_{2A} and A_{2B} receptors^{18–20}, opioid receptors^{21–23}, and recently cannabinoid receptors²⁴, metabotropic glutamate (mGlu) receptors¹² and A₁ receptors²⁵.

One of the limitations of this approach is the requirement of an affinity unit which is chemically compatible with the reactive moiety. For example, LD probes that include affinity units with nucleophilic functional groups (e.g. amine, thiol, phenol) may be chemically unstable due to the possible intra- and intermolecular reaction with the probe's reactive moiety, as it has previously reported²². To overcome these limitations, affinity-guided labelling with DMAP-catalysis or oxime-linked ligands have been proposed^{26,27}. Here we report an alternative approach, the click ligand-directed labelling (CLD), which may offer several advantages. In CLD, the labelling probe is generated by a fast click reaction between the chemically incompatible affinity unit and the reactive linker shortly before applying it to the native system in order to prevent side reactions (Fig. 1A, B).

In the present work, we describe the development and validation of a CLD approach to specifically and covalently attach fluorescent dyes to

endogenous GPCRs, maintaining the full functionality of the target receptor. In particular, our approach allows the labelling of dopamine receptor D₁, belonging to the class A aminergic GPCRs subfamily, which are commonly bound by ligands that possess nucleophilic groups, such as amines or phenols that may compromise the stability of the labelling probe. We have used an alternative modular approach that allowed us to build rapidly a labelling probe to minimise its intrinsic degradation and subsequently label the native D₁ receptor both within transfected cells as well as neuronal cell lines, which endogenously express D₁ receptor.

Results and discussion

Approach design and synthesis of the units

We aimed at labelling a native D₁ receptor with a fluorescent dye using a ligand-directed labelling probe. We selected dopamine D₁ as an archetypical aminergic class A GPCR, which is mainly expressed in the central nervous system (CNS). Its endogenous agonist is the neurotransmitter dopamine (DA), but many synthetic agonists and antagonists have been reported to date, including the agonists SKF38393 and SKF81297 and the potent antagonist SKF83566 (Fig. 1C). The latter has been already derivatised with different linkers looking for the best high affinity fluorescent and biotin probes²⁸. As reactive moiety of the LD probe, we selected the acyl imidazole, which preferentially labels lysine residues^{15,29}. However, the chemical nature of D₁ ligands is incompatible with LDAI for two reasons: (i) the secondary or tertiary amine can react with the acyl imidazole moiety or catalyse its hydrolysis and (ii) the phenol or catechol groups can react with the acyl imidazole.

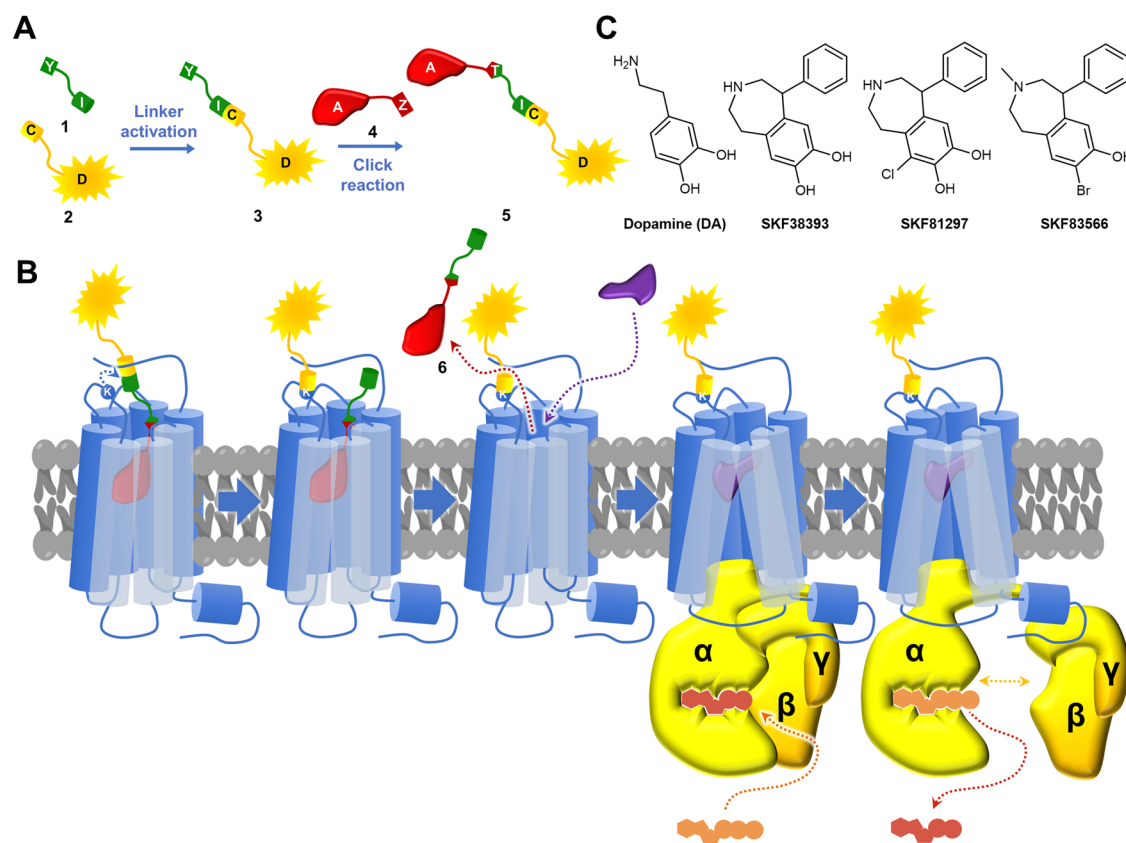
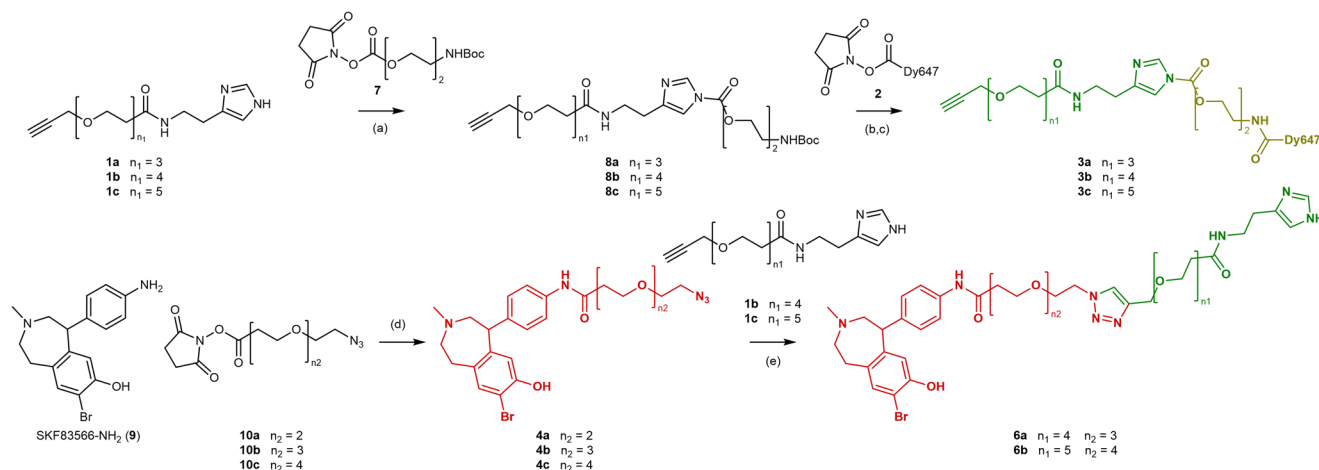


Fig. 1 | CLD labelling technology and ligands for the D₁ receptor. **A** Click ligand-directed approaches (CLD) can be used with nucleophilic affinity units and are prepared shortly before the labelling step. To prepare the labelling probes, an alkyne (Y) linker equipped an imidazole (I) terminal (1) is employed to activate an acyl group (C) linked to a fluorescent dye (D) (2) and thus forming the activated clickable dye (3). Compound 3 will be reacted through a click CuAAC reaction with compound 4, consisting of the ligand or affinity unit (A) linked to an azide (Z) terminus to form a triazole (T) and give the final labelling compound (5). **B** Click ligand-

directed (CLD) probes 5 bind to the target native GPCR and a lysine residue in can react with the imidazole-activated carboxylate (IC) of the linker. A covalent bond with the dye is formed and by-product 6 can be released and washed-out, leaving the native GPCR labelled and fully functional. Other agonists or antagonists (purple) will be able to bind the labelled receptor after the procedure. **C** Chemical structures of common agonists (Dopamine, SKF38393, SKF81297) and antagonists (SKF83566) of dopamine D₁ receptor.



Scheme 1 | Key synthetic steps for the synthesis of molecular modules **3**, **4** and **6**. Reagents and conditions: (a) Pyr 3.0 eq, DMF, 25 °C, 3 h, 27–79%; (b) TFA, 10 K eq, 30 min, (c) DIPEA 5.0 eq, DMSO, 25 °C, 1 h, 15–33% (two steps). (d) MeCN, 60 °C, 20–48 h, 21–60%; (e) Cu₂O 0.25 eq, BzOH 4.0 eq, THF/H₂O 1:4, rt, 0.5–1.5 h, 25–79%.

To avoid these problems, we decided to use a CLD labelling strategy (Fig. 1A, B) based on a heterogeneous copper(I)-catalysed azide-alkyne cycloaddition (CuAAC) chemistry, which was previously employed in native tissue photopharmacology³⁰ and is compatible with *in vivo* testing³¹. Hence, we employed different molecular modules: a clickable linker **1** equipped with an alkyne terminus (**Y**) and an imidazole (**I**), which is used to activate a carboxyl group (**C**) of the molecular module **2** containing a red fluorescent dye (**D**, Dy647) and form the activated module **3** (Fig. 1A). Next, the molecular module **4**, which consists of an affinity unit based on a D₁ antagonist (**A**) equipped with a linker with an azide terminus (**Z**), is used to react with the activated module **3** through CuAAC click chemistry and form the final labelling probe **5** (Fig. 1A). Upon binding of probe **5**, a nucleophilic lysine (**K**) of the receptor surface will attack the imidazole-activated carbonyl (**IC**) to form a stable covalent bond and thus label D₁ receptor (Fig. 1B). The labelling by-product **6** will be washed away, leaving the binding pocket unmodified and the receptor fully functional. Therefore, other ligands such as agonists, antagonists or even fluorescent antagonists will be able to bind the receptor after the labelling process (Fig. 1B).

Before synthesising the different molecular modules of the CLD labelling probe, we first analysed the amino acid sequence of D₁ receptor and its structure (obtained from GPCRdb^{32,33}). We identified the solvent-exposed lysines K165 and K167, which are located in the extracellular loop 2 (ECL2), as potential residues for reacting with an activated acyl-imidazole (Fig. S1). We examined the distance from the binding pocket to the target the extracellular lysines in the model but the considerable number of variables regarding the linker accommodation between loops ECL2 and ECL3 complicates the search for optimal linker geometry and length that may give a successful labelling probe **5** (Fig. S1). Therefore, we opted to explore flexible PEG linkers with different distances, through a combination of different lengths of the subunits **1** and **4** (Fig. 1A, Scheme 1).

The key steps of the synthesis of the CLD molecular modules are depicted in Scheme 1 and the detailed synthesis of the different subunits is described in the Supplementary Note S1. To prepare the fluorescent activated linkers **3**, we synthesised three clickable imidazole PEG linkers with di- tri- or tetra-ethylene glycol units, respectively, bearing an *O*-propargyl and a histamine carboxamide on each terminus respectively (**1a-c**, Scheme 1, Supplementary Note S1). As activated imidazole alkyl carbonyl compounds are reported to be unstable²⁹, we opted to add an extra linker to synthesise an activated imidazole carbonyloxy linkers as amine-reactive groups, which would modify the protein lysine residues by forming a carbamate group. This involves a three-step synthesis, starting from the preparation of the acylimidazoles **8a-c** from imidazole-containing clickable linkers **1a-c** and the NHS-activated carbonate with a Boc-protected amine **7** (Scheme 1, step a). Acidic deprotection of the Boc group gave an

intermediate amine, which reacted preferably with the fluorescent Dy647-NHS ester (**2**), to give the advanced molecular modules **3a-c** (Scheme 1, steps b-c).

To design the affinity unit, we selected the antagonist SKF83566 (Fig. 1C) due to its high affinity and selectivity for the D₁ receptor, which were considered likely to be retained after being modified with three different PEG-linkers (**4a-c**, Scheme 1), as high affinity D₁ ligands based on the modification of the SKF83566 structure are reported³⁴. First, the *para*-aniline analogue of SKF83566 (SKF83566-NH₂, **9**) was synthesised (Supplementary Note S1)³⁴ and acylated with an activated carboxylic acid with di- or tetra-ethylene glycol linkers, respectively, having a terminal azido group (**10a-c**) to give clickable PEG-ligands **4a-c** (Scheme 1, step d). Additionally, we prepared two imidazole ligands **6a-b**, corresponding to the by-products from the acyl-transfer reaction that yields to the desired labelled D₁-receptor (Fig. 1B). The study of their kinetic binding properties can be advantageous to anticipate the unbinding of the by-products **6** after the labelling reaction. Compounds **6a-b** were synthesised through a CuAAC click reaction from the corresponding azido ligand **4** and alkyne linker **1** (Scheme 1).

Pharmacological characterisation of the affinity units

Since affinity values cannot be determined for irreversible ligands such as compounds **5** and IC₅₀ values would vary over time, we characterised the pharmacological properties of the reversibly-binding analogues **4a-c** and **6a-b** upon the human D₁ receptor. This involved both functional and binding assays and was compared with the activity of the parent D₁ antagonist SKF83566 (Fig. 1C).

First, the antagonistic behaviour of compounds **4a-c** and **6a-b** was assessed using a functional HTRF[®] cAMP Gs Dynamic assay (Revvity) in HEK293 cells transfected with the human F-ST-D₁ receptor. Increasing concentrations of compounds SKF83566, **4a-c** and **6a-b** were able to inhibit the activation of D₁ induced by the agonist SKF38493 (300 nM) (Fig. 2A). Despite all compounds displaying inhibitory potencies in the nanomolar range, ligands equipped with the shorter PEG-linkers showed a higher potency, with SKF83566 showing a higher pK_i and **6b** being the least potent antagonist (Table 1, Fig. 2A). The binding properties of compounds SKF83566, **4a-c** and **6a-b** were assessed with Tag-*Lite*[®] assays (Revvity) with HEK293 cells, previously transfected with the human F-ST-D₁ receptor tagged with BG-Lumi4-Tb[®]. After performing saturation binding experiments with green D₁ antagonist (GDA, Revvity), we did kinetic association-competition binding assays with increasing concentrations of the D₁ antagonists and a constant concentration of GDA (120 nM), reading HTRF over a minimum of 60 min. From the obtained binding curves, the kinetic and equilibrium binding properties of each ligand were calculated, such as

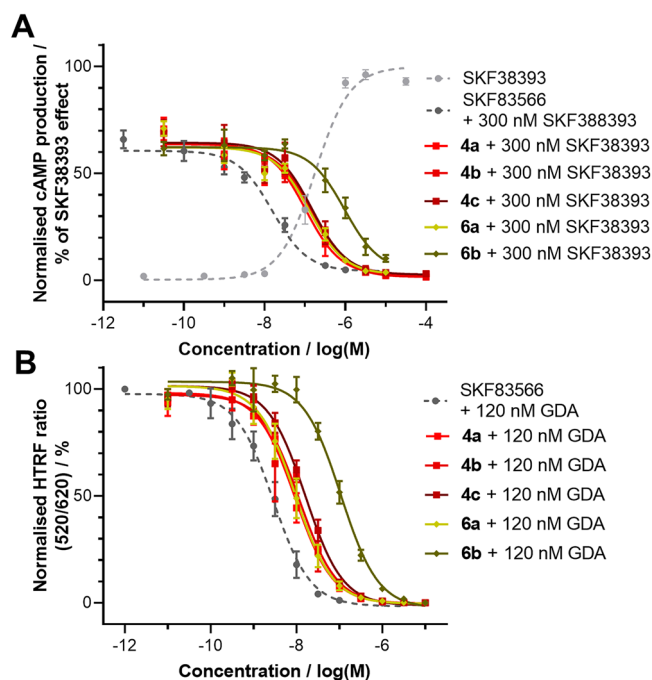


Fig. 2 | Pharmacological profile of units 4 and 6. **A** Functional concentration-response curves of **4a-c** and **6a-b** with a constant 300 nM concentration of the agonist SKF38393 using a cell-based HTRF[®] cAMP assay with F-ST-D₁. **B** Competition binding curves of **4a-c** and **6a-b** with a constant 120 nM GDA. Data points were extracted from cell-based Tag-Lite[®] association-competition binding assays and correspond to the means of a minimum of 3 independent experiments with the SEM shown as error bars. The error bars not displayed are smaller than data points.

the on-rate (k_{on}) and off-rate constants (k_{off}), residence time (RT) or dissociation constant (K_d) (Table 1, Fig. S2).

All ligands tested showed binding affinities in the nanomolar range with an inverse correlation of the linker length and binding affinity. All the ligands showed residence times in the same range (5–8 min), including the longer ligands **6a** and **6b**, which correspond to the labelling reaction by-products. These results indicate that, once the labelling probe is prepared and after receptor labelling, short times of perfusion are needed to wash-out the generated by-product **6** and leave the receptor binding site available. Additionally, the last six points of each binding curve were selected and plotted to obtain a competition concentration-response curve of each ligand. The inhibition constant (pK_i) values obtained from these curves were in line with the pK_d values obtained from the association-competition curves (Table 1, Fig. 2B). Interestingly, there is a shift of minimum 1.2 up to 1.5 log units between the binding affinity values (pK_d , pK_i) and the functional pK_i , probably due to the different nature of competition between agonist and antagonists.

Click reaction and receptor labelling

The final labelling probes **5a-i** were assembled immediately before application to the cells expressing human D₁ receptor, through a CuAAC click reaction between equimolar quantities of the of alkylnyl-dye **3a-c** and the azido-ligands **4a-c** (Fig. 3A) at 10–12 nmol scale in water in presence of Cu₂O (0.5–1.0 mg) and 4 mol-eq of benzoic acid. As expected, attempts to isolate reactive compounds **5** with an acceptable purity were unsuccessful, due to side reactions previously anticipated. To gain insight on this process, we monitored reaction progress by LC-PDA-MS and observed that the formation of the product **5h** is concomitant with the formation of hydrolysis products and a **5h**-isomeric product. The latter product was presumably originated from the intramolecular *O*-acylation reaction of the acidic phenol group (Fig. S3). Similarly, other phenol-containing LD labelling probes were similarly reported to have low chemical stability²². As

Table 1 | Pharmacological properties of compounds 4a-c and 6a-b

Compound	Functional	Binding (association-competition)		Binding (competition)
	$pK_i \pm \text{SEM}$	RT \pm SEM (min)	$pK_d \pm \text{SEM}$	$pK_i \pm \text{SEM}$
SKF83566	8.06 ± 0.10	5.6 ± 0.9	8.62 ± 0.14	8.71 ± 0.07
4a	7.38 ± 0.08	8.0 ± 1.2	8.10 ± 0.12	8.12 ± 0.11
4b	7.28 ± 0.17	5.0 ± 0.6	8.01 ± 0.08	8.13 ± 0.11
4c	7.20 ± 0.07	5.0 ± 1.0	7.94 ± 0.09	7.98 ± 0.07
6a	7.29 ± 0.21	7.5 ± 1.0	8.20 ± 0.10	8.20 ± 0.11
6b	6.36 ± 0.07	5.6 ± 1.2	7.26 ± 0.10	7.28 ± 0.12

The inhibition of D₁ functional activity by compounds **4a-c** and **6a-b** was assessed with a cell-based HTRF[®] cAMP Gs Dynamic assay with a constant 300 nM concentration of the agonist SKF38393. Cell-based Tag-Lite[®] association-competition binding assays were performed to obtain the kinetic binding properties of compounds **4a-c** and **6a-b** with F-ST-D₁. With the same assay the corresponding pK_i values were also obtained. Values are means of a minimum of 3 independent experiments with the corresponding standard error of the mean (SEM).

the isolation of the molecular probes **5** was impractical, we opted to directly use the resulting click-reaction mixture for receptor labelling after removing the Cu₂O by decantation and treatment with a copper-absorbing resin to prevent cytotoxicity associated to this metal²⁵.

To account for the competition of the specific affinity labelling of D₁ receptor and the non-specific reactions with other reactive molecules present in the cell system, CLD probes **5** were also incubated with an excess of 50 μM of SKF83566 to block probe binding to D₁ receptor. After a washing step, the specific labelling of the receptor was calculated by subtraction of the non-specific fluorescence readout from the total value. In addition, to discard the possibility that the signal obtained corresponds to unreacted probe **5** bound to the receptor, the cells were later incubated for 0.5 h with 50 μM of SKF83566 and washed. Thus, we were able to displace and remove any unreacted compound **5** and the reaction by-product **6** and, therefore, the measured total fluorescence corresponded only to the covalently labelled dye molecules (specific plus non-specific) produced by the chemical reaction with the CLD probes.

As a first step, we aimed to monitor the incubation time to optimise D₁ receptor labelling. Thus, we tested the labelling of F-ST-D₁ and HA-D₁ with **5e** as an intermediate-size CLD probe at five different concentrations with incubations of 0.5, 1, 2, 4 and 6 h. The SNAP-tag from F-ST-D₁ was co-labelled with Lumi4-Tb to read TR-FRET measurements and obtain a cleaner signal for the optimisation steps⁵. Since the Flag and the SNAP-tag[®] of F-ST-D₁ contain lysine residues that could be susceptible to labelling, the labelling experiments were performed in parallel with cells expressing HA-D₁, as HA-tag contains no lysine. Both results obtained with F-ST-D₁ reading HTRF and the Dy647-fluorescence obtained from HA-D₁ indicated that the incubations with micromolar concentrations of the reactive probe **5e** gave the maximum percentage of specific labelling after 2 h (Fig. S4). Additionally, we performed an in-gel fluorescence analysis on SDS-PAGE of fluorescently labelled receptors with CLD probe **5e**. We used HEK293 cells expressing F-ST-D₁, HA-D₁ receptor or F-ST-mGlu₅ receptor as a negative control. We observed fluorescent labelling in both constructs of D₁ receptor, but not for mGlu₅, confirming the selectivity of the labelling probe for the D₁ receptor (Fig. S5). We next tested the labelling properties of acyl imidazole CLD probes **5a-i** using the protocol at 2.5 h of incubation at different concentrations using both F-ST-D₁ and HA-D₁ (Fig. S6, S7, Table S1). Compound **5h** emerged as the CLD probe giving the best results, which includes an important separation between non-specific labelling and total labelling and a saturating behaviour of the specific labelling at high concentrations in HA-D₁-expressing cells (Fig. S7), consistent with site-specific labelling for D₁ receptor.

To further evaluate the labelling properties of compound **5h**, we aimed to determine the labelling amino acid residues involved in the labelling

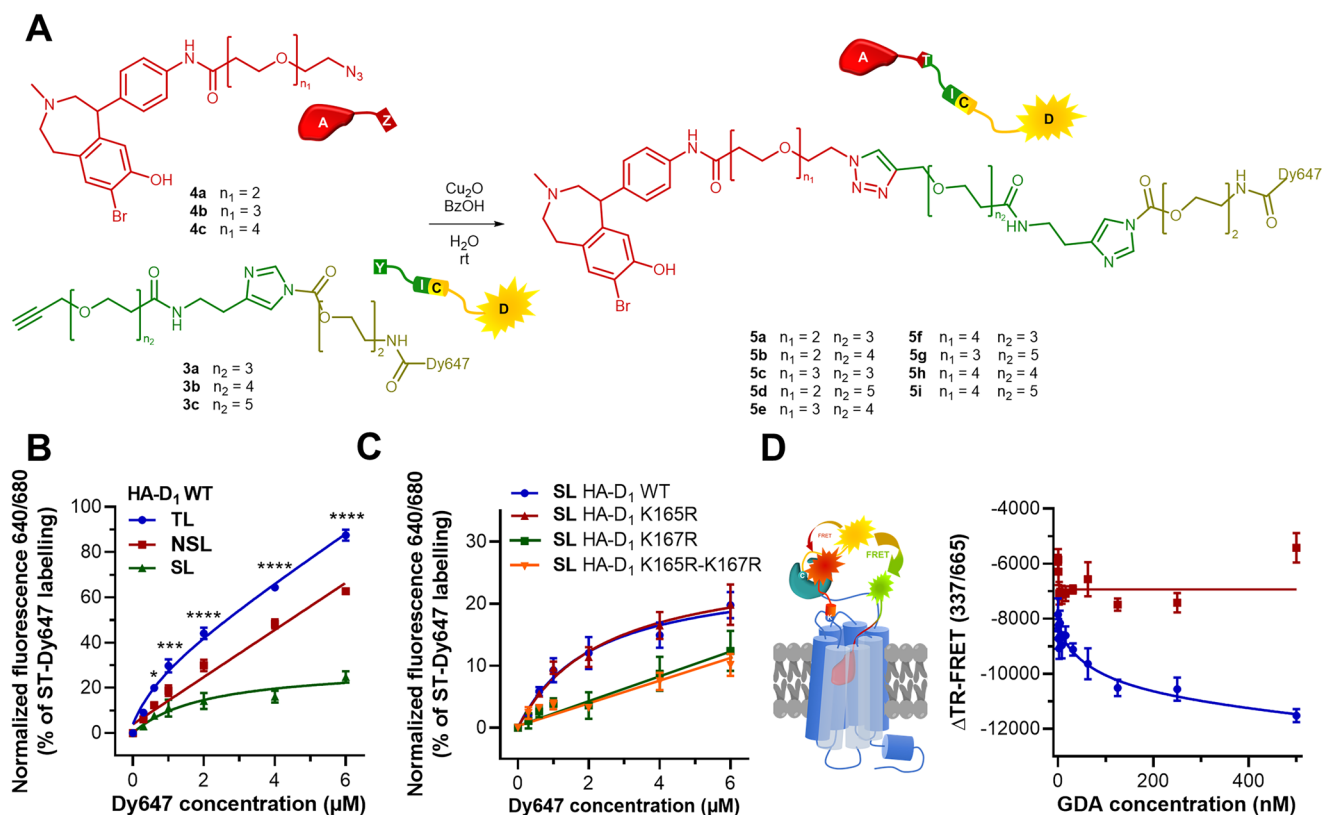


Fig. 3 | Click reaction to build the CLD labelling probe and labelling of D₁ receptor expressed in HEK293 cells. **A** The click reaction was performed combining compounds 3a–c with 4a–c to give the nine different combinations 5a–i. The concentration of compounds 3 and 4 was 200 µM in presence of 4 eq of BzOH and Cu₂O as catalyst. **B** The crude reaction of 5h was diluted and employed to label HA-D₁ with increasing concentrations from 0 to 6 µM (dye concentration) alone (total labelling, TL, blue dots) or in presence of 50 µM of the D₁ antagonist SKF83566, to measure the non-specific labelling (NSL, red dots and line). Subtraction of non-specific labelling from total labelling gave the specific labelling (SL, green dots and line). Data analysis show significant differences between total labelling and non-specific labelling values at 0.6, 1.0, 2.0, 4.0 and 6.0 µM using two-way ANOVA with Holm-Sidak correction for multiple comparisons (*0.05 < *p* < 0.01, ***0.001 < *p* < 0.0001, *****p* < 0.0001). **C** Compound

5h labelled specifically HA-D₁ WT, while it did not specifically label HA-D₁ K167R, indicating that K167 is the target residue for labelling. Data in graphs B and C correspond to the mean of three replicates performed in triplicate with the SEM as error bars. **D** Application of increasing concentrations of Green D₁ antagonist (GDA) in HEK293 cells expressing F-ST-D₁ labelled both with 5h and BG-Lumi4-Tb decreased the TR-FRET produced between Lumi4-Tb and the red dye labelled on K167 for cells non-treated with the antagonist SKF83566 (blue dots and line). This indicates that D₁ binding pocket GDA was bound to an unoccupied binding site. No decrease of TR-FRET was observed if the same cells were treated with the antagonist SKF83566 (i. e. with the binding site occupied) (red dots and line). The graph is a representative example of two replicates performed in quintuplet and error bars correspond to the SEM. The error bars not displayed are smaller than data points.

reaction. As the acyl-imidazole reactive moiety is reported to primarily target lysine residues^{14,15}, we prepared two constructs of HA-D₁ with a single point mutation of the extracellular solvent-exposed lysines with arginines (K165R, K167R) and one construct with the double mutation (K165R-K167R). We selected arginine as a replacing amino acid of lysine since it maintains the positive charge, and thus the structural properties of the lysine, but it has a higher pK_a, involving a decreased nucleophilicity towards acyl transfer reactions like labelling reaction with probe 5h. After verifying that the three mutants and wild type (WT) HA-D₁ are functionally equivalent (Table 1 and S2; Fig. S8), we performed the labelling experiments using the CLD labelling probe 5h with the four HA-D₁ constructs. In such experiments, we found it convenient to add a filtration step through a Durapore® PVDF filter (0.22 µm) after the click reaction and before the cell incubation. This helped to remove possible compound aggregates in the cell mixture, observed later by microscopy (Fig. S10), that could increase the non-specific fluorescence. In parallel, the F-ST-D₁ was labelled with BG-Dy647 to estimate the fluorescence corresponding to the totality of receptors expressed at the cell surface. The results showed significant differences between the total and non-specific labelling in most of the doses tested (Fig. 3B), thus confirming significant labelling of the wild type HA-D₁ receptor. In particular, we obtained 20 ± 2% of the D₁ receptors labelled at 6 µM concentration and B_{max} of 27 ± 3% (Fig. 3B) after fitting the different experimental points with a Langmuir isotherm function.

Interestingly, the mutated HA-D₁ K165R showed very similar labelling properties: 20 ± 3% of the receptors labelled at 6 µM and with a B_{max} 29 ± 8% (Fig. 3C, S9). This indicates that the involvement of Lys165 in the D₁ labelling is limited. HA-D₁ mutants K167R and K165R-K167R showed still some specific labelling, but substantially reduced compared to the wild type and K165R versions and the different concentration points did not fit well with a Langmuir function. This revealed that Lys167 plays an active role in the labelling reaction with the CLD probe 5h, pointing towards this amino acid as a likely preferential site of *N*-acylation reaction to obtain a fluorescently labelled D₁ receptor. Alternatively, the preferential labelling site could also be determined by proteomic techniques and MS spectroscopy, giving the possibility to identify secondary labelling residues, such as serines^{10,15}. Additionally, the possible off-target labelling responsible of part of the non-specific labelling could be determined by pull-down proteomics, as reported for other LD probes³⁶.

The LD strategies that we are developing are intended to leave the receptor fully functional, since the labelling by-product 6 can be washed-out and leave the binding site unoccupied. We checked this point by labelling HEK293 cells transiently expressing F-ST-D₁ with both the CLD probe 5h and BG-Lumi4Tb. Thus, upon excitation of the terbium cryptate labelled on the SNAP-tag³, part of the energy would be transferred to the red FRET acceptor (i.e. Dy647) labelled on Lys167, to produce fluorescence emission at 665 nm (i.e. TR-FRET)⁵. Next, the cells were treated with increasing

concentrations of green D₁ antagonist (GDA, Revvity) to interfere in the TR-FRET transfer between Lumi4Tb and Dy647 upon binding. Definitively, a decrease of the fluorescence emission at 665 nm was observed in the presence of GDA. Such decrease was fitted with a conventional saturation binding function (Figs. 3D, S8) allowing us to obtain the corresponding K_d (77 ± 53 nM), which was comparable with the K_d of GDA obtained in Tag-Lite[®] assays (184 ± 9 nM) (Fig. S2). In contrast, the double-labelled cells additionally treated with an excess of 50 µM of antagonist SKF83566, showed no decrease of red fluorescence upon GDA application (Figs. 3D, S8). This demonstrates that the orthosteric ligands such as GDA can bind to the D₁ receptors previously labelled with the CLD probe 5 h.

Visualisation of labelling of D₁ receptor

We visualised the Dy647 labelling of D₁ receptor by the probe 5 h in HEK293 cells using widefield microscopy. Shortly after the generation of the CLD probe 5 h by a click reaction (*vide supra*), we applied a 2.5 µM solution to living HEK293 cells transiently expressing a construct of D₁ receptor fused to a fluorescent protein (i.e. Myc-D₁-Venus). After the washing steps, the fluorescence of Dy647 was observed on the plasma membrane (Fig. 4A) in a similar manner to F-ST-D₁ with the SNAP-tag[®] labelled with BG-Dy647 (Fig. S10) and with a high degree of co-localisation ($R^2 = 0.8462$) between Dy647 and the intracellular Venus fluorescence (Fig. 4A, B). We did not observe specific labelling with the CLD probe 5 h in HEK293 cells not expressing the D₁ receptor. However, in the current experimental conditions, we still observed a minor non-specific labelling presumably coming from CLD aggregates dispersed in the culture (Fig. S10), which may be responsible of the non-specific signal observed in the fluorimeter (Fig. 3B). Additionally, the click reaction mixture excluding the clickable fluorescent module 3b did not affect the Venus fluorescence in Myc-D₁-Venus transfected cells, nor did it induce fluorescence in the red channel (Fig. S10). These data show a specific labelling of the D₁ receptor in living cells.

To exclude the interference of the lysine of the Myc-tag, we replaced it with HA-tag, which contains no lysine. Thus, we repeated the labelling procedure HA-D₁ and subsequently fixed the cells with paraformaldehyde (PFA). Again, the fluorescence of Dy647 was observed on the plasma membrane, with a high degree of co-localisation with anti-HA immunostaining fluorescence (Fig. 4C), confirming that CLD probes can be employed as reagents to visualise D₁ expression in cells. Additionally, incubation of HA-D₁-expressing cells with 5 h in competition with an excess of D₁-selective antagonist SKF83566 prevented D₁ labelling, indicating the need for an accessible D₁ binding site for the reaction to occur and the high specificity of the labelling process with our CLD probes for the D₁ receptor (Fig. S10).

Next, we aimed to visualise the organisation and dynamics of the D₁ receptor, such as monitoring the agonist-induced receptor trafficking. To achieve this, 5 h was applied to label HA-D₁ receptor expressed in the plasma membrane of HEK293 cells, which were also expressing a membrane marker fused to a green fluorescent protein (GFP) domain. First, we observed co-localisation of the fluorescence from GFP and the CLD labelling in the plasma membrane. Subsequently, we applied an excess of an orthosteric D₁ agonist (1 µM SKF81297, Fig. 1C) and we observed a significant decrease of the red fluorescence in the plasma membrane at different time points (Fig. 4D, S11) reaching 60–70% of the initial fluorescence. In contrast, upon vehicle addition, the red fluorescence remained over time. This indicates agonist-induced internalisation of a fraction of the CLD-labelled HA-D₁ receptors, which is in line with other reports in literature^{37,38}. Furthermore, these results were in line with DERET internalisation experiments on F-ST-D₁ receptor labelled with BG-Lumi4-Tb (Fig. S11)³⁹. This experiment further confirms that the binding site of CLD-labelled native D₁ remains fully functional, as the agonist efficiently induced a similar receptor trafficking to other established methodologies^{37–39}.

We then demonstrated that our approach allows the efficient labelling of endogenous D₁ receptors in their native environment. We used SH-SY5Y human neuroblastoma cells differentiated into viable neurons⁴⁰ that

endogenously express D₁ receptor. These cells were labelled with our CLD probe 5 h using the labelling protocol described above and imaged using widefield microscopy. We observed that CLD labelling co-localised with the fluorescence originating from immunostaining with an anti-D₁ antibody recognising the C-term of D₁ receptor. Note that the later stained D₁ receptors are located at both plasma membrane and intracellular compartments, in contrast to CLD labelling, which does not occur intracellularly (Fig. 4E). As a result, the fluorescence co-localisation is partial as it can only be observed at the plasma membrane (Pearson's $r = 0.69 \pm 0.03$, 14 cells, Fig. S12). Overall, we can confirm that CLD probe 5 h labels the endogenous D₁ receptor at the extracellular membrane of native D₁ receptor.

Conclusions

We developed a modular ligand-directed technology (CLD) to chemically label native D₁ receptor with fluorescent dyes as a proof of concept to possible label other aminergic receptors. CLD labelling is based on affinity reactive probes that can be prepared through a CuAAC click reaction shortly before the labelling reaction with the receptor. On the one hand, this modular chemical approach allows us to employ affinity units with nucleophilic substituents (such as D₁ or other aminergic GPCR ligands), since the final labelling probe is built immediately prior to labelling, preventing part of the intrinsic probe degradation. Additionally, the modular nature of our technology gives us the opportunity to extend the application of the molecular unit 3a-c to label other receptors or proteins of interest and construct a toolbox of ligand directed labelling probes for clinically relevant target proteins. This requires only the development and optimisation of a module corresponding to the affinity unit 4, which needs to be specific for the new protein of interest and include a linker that can accommodate between the binding pocket and the solvent exposed area to properly direct a labelling reaction.

We have obtained a moderate labelling yield when compared with well-established technologies on engineered receptors, such as SNAP-tag[®] labelling, but this work represents a proof of concept of how to overcome the pitfall of labelling endogenous aminergic GPCRs without the need for genetic engineering. To that end, we used the CLD probe 5 h, which includes an established electrophilic group in ligand-directed labelling (i.e. acyl imidazole) and directs the N-acylation reaction to Lys167, as proven by mutagenesis. Other electrophilic species, such as SP or NASA already used in LD labelling¹⁰, can be used in the future to improve both the residue specificity, reaction rates and reduce of the non-specific labelling. Additionally, we do not discard in future approaches the possibility to employ copper-free click chemistry such as strain-promoted azide-alkyne cycloaddition (SPAAC) or the faster inverse electron-demand Diels-Alder reactions (IEDDA)^{41,42}, which involve bulkier functional groups. In this situation, an optimisation of the substitution pattern and linkers will be necessary to assure the water-solubility of the probe and a correct probe positioning upon binding to the receptor.

Despite the moderate labelling yield, the presented CLD approach allowed us to visualise the HA-D₁ receptor expressed in the plasma membrane of HEK293 cells or endogenous D₁ in neuron-like differentiated cells. The technology here presented can provide tool compounds in chemical biology to develop a great variety of reagents to be employed in the field of native GPCR research, in part, because the binding site remains unaltered after labelling and can accommodate other orthosteric ligands, as we have demonstrated using TR-FRET experiments. Additionally, we were able to monitor the internalisation of D₁ upon agonist application and demonstrated once more that the binding site of the CLD-labelled receptor remains unaltered and the receptor is functional after labelling, as agonists could bind and induce receptor internalisation. This was one example of possible applications but multiple other choices could be explored such as monitoring receptor dynamics or partnering between proteins. These may include the study of protein-protein interactions in endogenous tissues using FRET between fluorophores covalently conjugated to different native proteins and a possible translation of the Tag-Lite[®] technology to native receptors and eventually in tissue samples, organs and in vivo.

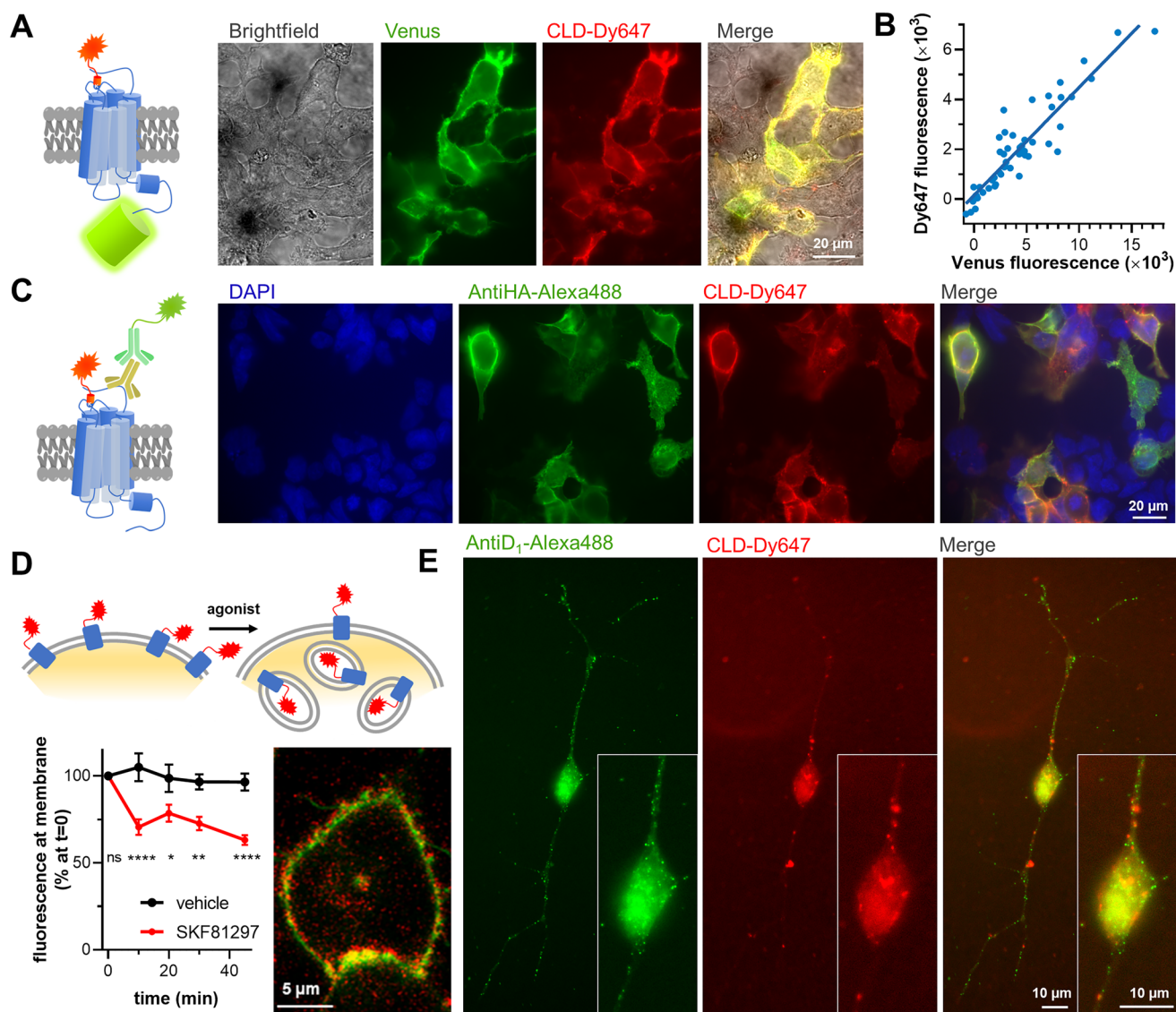


Fig. 4 | Visualisation of D₁ receptors labelling with CLD labelling probe 5 h. **A** Widefield microscopy image of live HEK293 cells transiently expressing Myc-D₁-Venus. The cells were treated with CLD probe 5 h (2.5 μM), washed four times and imaged. Venus and Dy647 fluorescence originated from labelling with 5 h were located mostly at the cell membrane with a high degree of co-localisation (**B**) $R^2 = 0.8462$. **C** Widefield microscopy image of five HEK293 cells transiently expressing HA-D₁ were labelled with 5 h using the same protocol, fixed with PFA, immunostained and imaged. Immunostaining fluorescence (AntiHA-Alexa488) and CLD fluorescence (CLD-Dy647) were located mostly at the cell membrane with a high degree of co-localisation (Merge). **D** Evolution of the 680-nm membrane fluorescence of living HEK293 cells transiently expressing membrane marker fused

to GFP and HA-D₁ labelled with 5 h after agonist SKF81297 (1 μM) application, as a result of receptor trafficking analysed by confocal microscopy. Data are means ± SEM of nine cells. Data analysis show significant differences between agonist and vehicle treated cells at time using two-way ANOVA with Sidak correction for multiple comparisons (ns non-significant, *0.05 < p < 0.01, **0.01 < p < 0.001, **** p < 0.0001). **E** Widefield microscopy image of SH-SY5Y cells differentiated to neuron-like cells, which were labelled with 5 h using the same protocol, fixed with PFA, permeabilised, immunostained and imaged. Immunostaining fluorescence (left) and Dy647 fluorescence (centre) were located mostly at the cell membrane with a moderate degree of co-localisation (right). The error bars not displayed are smaller than data points.

Methods

Synthesis materials and methods

Unless mentioned otherwise, all reactions were performed under N₂ or Ar atmosphere. All chemicals and solvents were obtained from commercial suppliers (primarily Merck/Sigma-Aldrich, TCI, ABCR, Scharlau, Panreac, Fluorochem and Apollo Scientific) and used without purification. DCM, DMF, THF and toluene were dried by passing through a PureSolv solvent purification system. Compounds **1–33** were synthesised according to the procedures detailed in Supplementary Note S1. Dy647-NHS (**2**) was purchased from Dymomics. Reactions were monitored by thin layer chromatography (Macherey-nagel ALUGRAM SIL G/UV₂₅₄) by visualisation under 254 nm lamp or under revelation with phosphomolybdic acid or permanganate. Flash column chromatography was performed manually

with Silica Gel 60 (40–63 μm, PanReac) or automated with SNAP KP-Sil (50 μm, Biotage), SNAP KP-C18-HS (50 μm, Biotage) cartridges on Isolera One with UV-Vis detection (Biotage) or Grace Reveleris® Silica Flash cartridges (Büchi) with a Pure C850 FlashPrep with UV and light scattering detection (Büchi). Preparative HPLC was included a pump LC8A, UV detector SPD20A and a controller CBM20 A (Shimadzu) and a column Waters XBridge C18 - 5 μm - 19 × 100 mm. Nuclear magnetic resonance (NMR) spectra were determined with and on a 400 MHz Bruker Avance NEO instrument. Chemical shifts are reported in parts per million (ppm) against the reference compound using the signal of the residual non-deuterated solvent (CDCl₃ δ = 7.26 ppm (¹H), δ = 77.16 ppm (¹³C); DMSO δ = 2.50 ppm (¹H), δ = 39.52 ppm, (¹³C); CD₃OD δ = 2.50 ppm (¹H), δ = 39.52 ppm). NMR spectra were processed using MestreNova

10.0.2 software (Mestrelab Research). The peak multiplicities are defined as follows: s, singlet; d, doublet; t, triplet; q, quartet; dd, doublet of doublets; ddd, doublet of doublets of doublets; dt, doublet of triplets; dq, doublet of quartets; td, triplet of doublets; tt, triplet of triplets; br, broad signal; m, multiplet; app, apparent. All NMR spectra are depicted in Supplementary Data 1. Purity determination was performed with Liquid Chromatography (LC) coupled to a photodiode detector (PDA) and a mass spectrometer (MS). Three different equipment with different methods have been used and are described as followed. (LC1) Waters 2795 Alliance separation module coupled to a diode array detector (Agilent 1100) scanning at a wavelength range of 210–600 nm and an ESI Quattro Micro MS detector (Waters) in positive mode with mass range (m/z) of 150–1500. A column ZORBAX Extend-C18 3.5 μm 2.1 x 50 mm (Agilent) at 35 °C was used with a mixture of A = H_2O + 0.05% formic acid and B = MeCN + 0.05% formic acid as mobile phase and the method as follows: flow 0.5 mL min^{-1} , Gradient $t = 0.0$ min 5% B, $t = 0.5$ min 5% B, $t = 5.5$ min 100% B, $t = 7.0$ min 100% B, $t = 8.0$ min 5% B, $t = 10.0$ min 5% B, total runtime: 10 min. (LC2) Thermo Ultimate 3000 SD (Thermo Scientific Dionex) separation module coupled to a photodiode array detector scanning at a wavelength range of 190–950 nm and a mass spectrometer LTQ XL ESI-ion trap (Thermo Scientific) in positive mode with a mass range (m/z) of 150–1500. A column ZORBAX Extend-C18 3.5 μm 2.1 x 50 mm (Agilent) was used at 35 °C was used with a mixture of A = H_2O + 0.05% formic acid and B = MeCN + 0.05% formic acid as mobile phase and the method as follows: flow 0.9 mL min^{-1} , gradient: $t = 0.0$ min 5% B, $t = 0.0$ min 5% B, $t = 3.0$ min 100% B, $t = 6.0$ min 100% B, $t = 7.0$ min 5% B, $t = 10.0$ min 5% B, total runtime: 10 min. (LC3) UHPLC Acquity H Class equipped with Water SQD2 apparatus simple quadrupole by electrospray ionisation and PDA diode array detector (Waters). A column Acquity C18 1.7 μm – 2.1 x 50 mm (Waters) at 40 °C was used with a mixture of A = H_2O + 0.1% formic acid and B = MeCN + 0.1% formic acid as mobile phase and the method as follows: flow 0.6 mL/min, Gradient $t = 0.0$ min 10% B, $t = 7.5$ min 60% B, total runtime: 7.5 min. LC chromatograms and the corresponding MS spectra are depicted in Supplementary Data 2. High resolution mass spectra (HRMS) and elemental composition were analysed by FIA (flux injected analysis) with Ultrahigh-Performance Liquid Chromatography (UPLC) Aquity (Waters) coupled to LCT Premier Orthogonal Accelerated Time of Flight Mass Spectrometer (TOF) (Waters). Data from mass spectra were analysed by electrospray ionisation in positive and negative mode. Spectra were scanned between 100 and 1500 Da with values every 0.2 s and peaks are given m/z (% of basis peak). Data was acquired with MassLynx software version 4.1 (Waters) and analyses were performed at the mass spectroscopy service of IQAC-CSIC.

cDNA plasmids

The pRK5 plasmid encoding the wild-type human DRD1 (GenBank X55760.1) was generated by subcloning the synthetic human DRD1 gene sequence supplied by GeneCust (Ellange, Luxemburg) using engineered restriction enzyme sites EcoRI and XbaI. This sequence included a MluI site engineered after the start codon. DRD₁ was cloned into a pRK5 vector containing the sequences of the signal peptide (SP) of the mGlu₅ receptor, and of a Flag tag and a SNAP-tag, using the unique restriction sites for MluI and XbaI in the 5'- and 3'-terminal respectively to obtain the fused Flag-SNAP-hD₁. In a similar manner, DRD1 was cloned into a vector containing the sequence of the signal peptide (SP) of the mGlu₅ receptor and of a HA-tag using the same restriction sites to obtain HA-hD1.

Single point mutants K165R, K167R and double mutant K165R and K167R for both F-ST-D1 and HA-D1 were prepared by subcloning a synthetic gene supplied by GeneCust that encodes the first 209 amino acids and includes the desired mutations and a SpeI (ACTAGT) restriction site at the position 169 and 170. The final vector was made using the unique restriction sites for MluI and MscI of pRK5 plasmids F-ST-hD1 or HA-hD1, the preparation of which is described in the previous paragraph.

Myc-D1-Venus was obtained using standard molecular biology protocols employing fragment replacement and PCR approaches⁴³. The plasmid encoding the membrane marker fused to GFP (i.e. pcDNA3.1-rGFP-

CAAX) was obtained by PCR amplification of the sequence coding rGFP with a reverse primer encoding a linker (GSAGTMAASNTASG) and the PM-targeting sequence: GKKKKKKSKTKCVIM. The CAAX-targeting sequence is located at the C terminus of the sequence rGFP⁴⁴.

Cell culture, transfection and cell preparation

HEK293 cells (ATCC, Cat# CRL-1573) were cultured in DMEM (Life Technologies, Invitrogen) supplemented with 10% fetal calf serum (Lonza). Cells were transfected by the reverse Lipofectamine 2000 protocol described previously with a ratio DNA (μg)/LipofectamineTM2000 (μL) mix 0.3–0.4 in 96-well plates⁴⁵. Briefly, 100 000 cultured cells in 100 μL of DMEM were added in each well pre-coated with polyornithine, followed by 50 μL DNA-lipofectamine mix (preincubated for 20 min at rt) and the cells were incubated at 37 °C in a CO₂ incubator for 24 h. A total of 0.15 μg of DNA was incubated with 0.375 μL of LipofectamineTM 2000 in 50 μL Opti-MEM (1x) (Invitrogen) per well.

For T25 culture flasks, approximately 6 million cells in 2.4 mL DMEM (10% FVS) were incubated with 1.6 mL of DNA-lipofectamine mix (preincubated for 20 min at rt), which included 4 μg of DNA and 10 μL of LipofectamineTM 2000.

For 35 mm glass bottom dishes (MatTek[®]) pre-coated with polyornithine, approximately 2 million cells in 1.2 mL DMEM (10% FVS) were incubated with 0.8 mL of DNA-lipofectamine mix (preincubated for 20 min at rt), which included 2 μg of DNA and 6 μL of LipofectamineTM 2000.

For Tag-Lite[®] binding experiments, the same transfection was performed 150 mm culture dishes. Approximately 10 million cells in 12 mL DMEM were incubated 33 h with 8 mL of DNA-lipofectamine mix (preincubated for 20 min at rt), which included 20 μg of DNA and 65 μL of LipofectamineTM 2000. The cells were carefully washed with 10 ml PBS and 15 mL of a solution of SNAP-Lumi4-Tb^{*} (100 nM) in Tag-Lite[®] buffer was carefully added. The cells were incubated 90 min at 37 °C and 5% CO₂. The labelling buffer was removed and the cells were carefully washed with Tag-Lite[®] buffer (3 x 10 mL). Gibco[™] Cell-dissociation buffer (life technologies) was added (5 mL) and it was incubated 6 min at 37 °C and 5% CO₂. Tag lite buffer was added (20 mL) and the cells were collected, centrifuged at 1000 rpm and re-suspended in DMEM (10%FVS + 10%DMSO) to have 2 million cells per mL and store at –80 °C.

Pharmacology materials and methods

All pharmacology data is available in Supplementary Data 3.

Materials. Compounds **4a**, **4b**, **4c**, **6a** and **6b** were synthesised (Supplementary Note S1). D₁ ligands SKF38393 and SKF83566 were purchased from Tocris Bioscience. HTRF cAMP Gs Dynamic kit, SNAP-Lumi4-Tb^{*}, Green D₁ antagonist (GDA) and Tag-Lite[®] buffer were obtained from Revvity.

Functional HTRF[®] cAMP assay. The functional assays were performed using a HTRF cAMP Gs Dynamic assay (Revvity) following the recommendations of the manufacturer. Briefly, HEK293 cells transiently expressing D₁ receptor in 96-well plates were preincubated for 10 min with 37.5 μL of DMEM containing 500 μM of IBMX and the antagonists to be tested (1.25x, if necessary). The corresponding agonist solutions (4x, 12.5 μL) (i.e. SKF38393) were added and the cells were incubated between 20 and 30 min at 37 °C and 5% CO₂. 25 μL of solution of cAMP-d2 (1x) in HTRF cAMP lysis buffer and 25 μL of Anti-cAMP-Eu (1x) in HTRF cAMP lysis buffer were added in each well. The complexes were left 1 h at rt and the HTRF ratio was read with a Pherastar plate reader (BMG Labtech). The resulting HTRF ratio was transformed to produced cAMP using a standard curve as recommended by the manufacturer and the data was analysed using Prism 8 (Graphpad).

Binding Tag-Lite[®] assays. The binding properties of compounds **4a**, **4b**, **4c**, **6a** and **6b** were determined through association-competition binding assays using the Green D₁ antagonist (GDA, Revvity) using a

methodology previously described with membranes in 384-well⁸. Briefly, 12 increasing concentrations of the antagonists were placed in the plate together GDA (120 nM) in Tag-Lite[®] buffer. Also, 6 increasing concentrations of GDA were added to determine the binding properties of GDA and, in parallel, the same concentrations of GDA with a constant concentration 50 μ L of SKF83566 to determine the non-specific binding. A vial of 2 million cells expressing F-ST-D₁ labelled with SNAP-Lumi4-Tb[®] at -80 °C was thawed, centrifuged and the cell pellet was resuspended in 1 mL of Tag-Lite[®] buffer. 5 μ L of the cell suspension (10000 cells) were added in each well and the plate was read with Pherastar (BMG Labtech) with a kinetic programme reading HTRF at 520/620 mode every minute during 60–80 min. The data and was analysed using Prism 8 (Graphpad). Since a drift on the HTRF ratio was observed (probably due to photobleaching), the functions of association kinetics and competitive binding kinetics were adapted to account for the signal drift^{46,47}.

DERET internalisation assay. The internalisation of D₁ upon SKF81297 was monitored using HEK293 ATCC cells transiently expressing F-ST-D₁ in white 96-well plates as described above (3.4). 24 h after transfection, cells were labelled with 50 μ L of 100 nM of BG-Lumi4-Tb and incubated for 1 h at 4 °C. After the labelling period, cells were washed with 100 μ L of 1x Tag-lite buffer twice and receptor expression was measured in PHERAstar detection system (BMG Labtech) by directly measuring fluorescence at 620 nm after an excitation at 337 nm. Compounds were then added at the indicated concentrations together with 25 μ M fluorescein. The signal at 620 nm was recorded every 15 min during 60 min at 37 °C in PHERAstar detection system and plotted as a function of time.

CLD probe 5 preparation, receptor labelling and fluorescence reading

Materials. Compounds **3a**, **3b**, **3c**, **4a**, **4b** and **4c** were synthesised (vide supra). D₁ ligand SKF83566 were purchased from Tocris Bioscience. Benzoic acid (BzOH), copper oxide (I) (Cu₂O) and Durapore[®] PVDF filters (0.22 μ m) were purchased from Merck/Sigma-Aldrich. Tag-Lite[®] buffer, Lanthslider buffer and SNAP-Lumi4-Tb[®] (i.e. BG-Lumi4-Tb) was from Revvity. CupriSorb[™] (Seachem) resin was purchased from Amazon.

CLD probe 5 preparation. A solution of BzOH 1 mM (75 μ L) in milli-Q water was added in a tube containing 15 mmol of compound **4** and stirred 20 min with at 1200 rpm and 25 °C to obtain a solution 200 μ M. Add around 0.8–1.2 mg of Cu₂O in a vial containing 12 mmol of compound **3**. Recently prepared solution of compound **4** 200 μ M in BzOH 1 mM (60 μ L) was added in the tube containing compound **3** and Cu₂O and stirred 3 h with at 1000 rpm and 25 °C. Lanthslider buffer (540 μ L) was added to obtain a solution 20 μ M of the click product and the tube was centrifuged at 10000 rcf for 5 min. The resulting solution containing the CLD probe **5** (595 μ L) was taken carefully without dragging the insoluble Cu₂O and was added into a tube with around 1/3 of the volume with CupriSorb[™] resin and stir 20 min with a thermomixer at 1000 rpm and 25 °C. The maximum volume possible was taken without the CupriSorb[™] resin. As absolute concentration of the reactive probes **5** is never constant as it is evolving during time, the Dy647 concentration of the resulting solution was verified by UV-Vis absorption spectrophotometry ($\epsilon = 250000 \text{ M}^{-1} \text{ cm}^{-1}$), since it will remain constant. The solution was diluted with Lanthslider buffer to obtain the desired dye concentration.

Monitoring of click reaction to obtain probe **5 h.** Water (92 μ L) was added on vial containing 20 nmol of compound **3b**, a non-reactive internal standard containing Dy647 (Fig. S3) and Cu₂O (1,2 mg, 8,39 μ mol) and a solution of BzOH 5 mM (4,00 μ L, 0,020 μ mol). Next, a solution of compound **4c** (4,00 μ L, 0,020 μ mol) 5 mM and BzOH 20 mM (4,00 μ L, 0,080 μ mol). The resulting solution with Cu₂O

suspended was stirred at 1500 rpm at rt. Samples were taken for LC analysis at time points 0, 30, 60, 90, 120, 165, 210, 255, 300 min. Samples were prepared from 8 μ L of the reaction solution diluted with 8 μ L of MeCN and 16 μ L of water + 0.1% formic acid. The LC/MS method used was based on LC1 general method with a different gradient: 0–1 min 10%B 1–14 min 10–50%B 14–16 min 50–100%B 16–18 100%B 18–19 min 10%B 10B 19–20 10%B total runtime 20 min and a scanning at a wavelength range of 210–700 nm for the diode array detector.

Receptor labelling. The medium of cultured HEK293 cells expressing D₁ was removed and washed with PBS. A solution of CLD probe **5** with the desired concentration was added and the cells were incubated during 2.5 h at 37 °C and 5% CO₂. To determine the non-specific labelling, the solution of CLD probe **5** also contained 50 μ L of SKF83566. The medium was removed and the cells were washed four times with Lanthslider buffer waiting 5 min between washes. The fluorescence 640/680 ratio was read with a Pherastar plate reader (BMG Labtech) and the data was analysed using Prism 8 (Graphpad). To confirm that the data obtained from the cell fluorescence was due to covalent labelling, the cells were incubated with 50 μ L of SKF83566 in Lanthslider buffer for 0.5 h at 37 °C and 5% CO₂. The cells were washed 3 times with Lanthslider buffer, the fluorescence 640/680 ratio was read again with a Pherastar plate reader (BMG Labtech) and the data was analysed using Prism 8 (Graphpad). Total labelling and non-specific labelling were fitted to a one-site *total and non-specific* saturation binding curves. Subtraction of non-specific labelling from total labelling gave the specific labelling and was fitted to a one-site *specific* saturation binding curves. Labelling data is available in Supplementary Data 4.

Gel fluorescence analysis on SDS-PAGE. The medium of cultured HEK293 cells expressing HA-D₁, F-ST-D₁ or F-ST-mGlu₅ was removed and washed with PBS. The cells were incubated for 6 h at 37 °C and 5% CO₂. with a solution 4 μ M of CLD probe **5** in Lanthslider buffer. Control cells were also labelled with 250 nM solution of SNAP-Dy647 or SNAP-Dy782 in Lanthslider buffer. The medium was removed and washed with Lanthslider buffer at 37 °C 4 times and the cells were incubated at 4 °C for 20 min *N*-ethylmaleimide (25 mg in 10 ml). The wells were washed with 1 mL of cold PBS and incubated with mild orbital shaking at 4 °C for 46 min with a protease inhibitor solution in RIPA Lysis buffer (50 mM TrisHCl, pH 7.4; 150 mM NaCl ; 1% Nonidet P-40 ; 0.5% sodium deoxycholate ; 0.1% SDS + PI). The soluble fraction was transferred to a fresh tube and centrifuged the tubes 12 000 g for 30 min at 4 °C. 20 mL of the supernatant containing the membranes was treated with 5 μ L of NuPAGE sample buffer (Invitrogen) and heated at 37 °C for 10 min. 21 μ L of the resulting solution was and 7 μ L of Invitrogen marker were loaded in each well of a 10-well NuPAGE gel 3–8% Tris-Acetate (Invitrogen), which was in the corresponding running buffer (40 mL 20X NUPAGE Tris-Acetate SDS Running Buffer + 760 mL H₂O). The gel was run at 150 V constant for 90 min. The gel was scanned directly using the 700 nm channel for Dy647 reading and the 800 nm for Dy782 reading of the Odyssey Infrared Imaging System (LI-COR Biosciences).

Receptor labelling and TR-FRET binding experiment to determine binding site occupancy. HEK239 cells expressing human F-ST-D₁ cultured in a T25 flask were labelled with a solution of CLD probe **5** (2 mL, 5 μ M, see 3.6.2) containing 100 nM of SNAP-Lumi4-Tb[®] and the cells were incubated during 2.5 h at 37 °C and 5% CO₂. The labelling buffer was removed and the cells were carefully washed with Tag-Lite[®] buffer waiting 5 min between washes. Gibco[™] Cell-dissociation buffer (life technologies) was added (3 mL) and it was incubated 6 min at 37 °C and 5% CO₂. Tag lite buffer was added (2 mL) and the cells were collected, centrifuged at 1000 rpm and re-suspended in Tag-Lite[®] buffer to have 2 million cells per mL of double labelled SNAP-Lumi4Tb and CLD Lys167-Dy647.

In a similar manner than in Tag-Lite® binding experiments, 12 increasing concentrations of GDA were added and, in parallel, the same concentrations of GDA with a constant concentration 50 µL of SKF83566 to determine the non-specific binding. 10 µL of the cell suspension (20000 cells) were added in each well, the plate was immediately read with Pherastar (BMG Labtech) with TR-FRET at 337/665 mode, the cells were incubated 60 min at 37 °C and 5% CO₂ and the plate was read again with Pherastar (BMG Labtech) with TR-FRET at 337/665 mode. The difference of TR-FRET was analysed using Prism 8 (Graphpad).

Microscopy methods and materials

D₁ receptors labelling with CLD probe 5 h 2.5 µM was performed as described above. Cells were either fixed using paraformaldehyde 4% during 15 min for immunocytochemistry, or not fixed for live imaging (performed 2.5 to 4 h after D₁ labelling with CLD).

Immunocytochemistry was performed on 0.1% Triton 100X permeabilised cells after blocking unspecific binding site with 15 min 2% PBS/BSA solution incubation. Incubation with primary and secondary antibody (rat anti-HA (11867423001, Sigma)), rat anti-D₁ (D2944, Sigma) and donkey anti-rat Alexa 488 (712-545-150, Jackson ImmunoResearch) diluted in 2% PBS/BSA solution was done overnight at 4 °C and 1h30 at room temperature, respectively. Cells were then labelled with Hoescht (15–30 s of labelling) and dako mounting medium was applied before covering cells with a glass coverslip for hours at room temperature.

Widefield images were acquired with an Axio-Observer 7 microscope (Zeiss) equipped with the ORCA-Flash4 camera (Hamamatsu), 63X Plan Aplanachromat objective (ZEISS, 1.4 NA, oil), transmitted light (tungsten 100 W LED), FTIC (Ex. BW: 470/40 nm – Dichroic FT 495 – Em. BW: 525/50 nm [n°32 Zeiss], 0.5 s exposition time) and Cy5 (Ex. BW: 665/45 nm – FT 695 – BW 725/50 nm [n° 38 Zeiss], 5 s exposition time) filters.

Confocal images were acquired with a Zeiss LSM980 microscope equipped with airyscan. Objective 40 × 1.3. Lasers : excitation 488 with detection 500-560 and excitation 633 with detection 650-720.

Microscopy data is available in Supplementary Data 5.

Reporting summary

Further information on research design is available in the Nature Portfolio Reporting Summary linked to this article.

Data availability

The data supporting this article have been included in the Supplementary information, Supplementary Data 1–5 and it is available from the corresponding author on reasonable request.

Code availability

This manuscript does not report original code.

Received: 14 October 2024; Accepted: 24 March 2025;

Published online: 11 April 2025

References

1. Sriram, K. & Insel, P. A. GPCRs as targets for approved drugs: how many targets and how many drugs? *Mol. Pharmacol.* **93**, 251–258 (2018).
2. Stoddart, L. A. et al. Application of BRET to monitor ligand binding to GPCRs. *Nat. Methods* **12**, 661–663 (2015).
3. Kauk, M. & Hoffmann, C. Intramolecular and intermolecular FRET sensors for GPCRs – monitoring conformational changes and beyond. *Trends Pharmacol. Sci.* **39**, 123–135 (2018).
4. Lang, K. & Chin, J. W. Cellular incorporation of unnatural amino acids and bioorthogonal labeling of proteins. *Chem. Rev.* **114**, 4764–4806 (2014).
5. Zwier, J. M., Bazin, H., Lamarque, L. & Mathis, G. Luminescent lanthanide cryptates: from the bench to the bedside. *Inorg. Chem.* **53**, 1854–1866 (2014).
6. Scholler, P. et al. Time-resolved Förster resonance energy transfer-based technologies to investigate G protein-coupled receptor machinery: high-throughput screening assays and future development. *Prog. Mol. Biol. Transl. Sci.* **113**, 275–312 (2013).
7. Zwier, J. M. et al. A fluorescent ligand-binding alternative using tag-lite® technology. *J. Biomol. Screen.* **15**, 1248–1259 (2010).
8. Sykes, D. A. & Charlton, S. J. Single step determination of unlabeled compound kinetics using a competition association binding method employing time-resolved FRET. *Methods Mol. Biol.* **1824**, 177–194 (2018).
9. Takaoka, Y., Ojida, A. & Hamachi, I. Protein organic chemistry and applications for labeling and engineering in live-cell systems. *Angew. Chem. Int. Ed.* **52**, 4088–4106 (2013).
10. Tamura, T. & Hamachi, I. Chemistry for covalent modification of endogenous/native proteins: from test tubes to complex biological systems. *J. Am. Chem. Soc.* **141**, 2782–2799 (2019).
11. Shiraiwa, K., Cheng, R., Nonaka, H., Tamura, T. & Hamachi, I. Chemical tools for endogenous protein labeling and profiling. *Cell Chem. Biol.* **27**, 970–985 (2020).
12. Nonaka, H. et al. Bioorthogonal chemical labeling of endogenous neurotransmitter receptors in living mouse brains. *Proc. Natl Acad. Sci. USA.* **121**, e2313887121 (2024).
13. Tsukiji, S., Miyagawa, M., Takaoka, Y., Tamura, T. & Hamachi, I. Ligand-directed tosyl chemistry for protein labeling in vivo. *Nat. Chem. Biol.* **5**, 341–343 (2009).
14. Miki, T. et al. LDAO-based chemical labeling of intact membrane proteins and its pulse-chase analysis under live cell conditions. *Chem. Biol.* **21**, 1013–1022 (2014).
15. Fujishima, S. H., Yasui, R., Miki, T., Ojida, A. & Hamachi, I. Ligand-directed acyl imidazole chemistry for labeling of membrane-bound proteins on live cells. *J. Am. Chem. Soc.* **134**, 3961–3964 (2012).
16. Takaoka, Y., Nishikawa, Y., Hashimoto, Y., Sasaki, K. & Hamachi, I. Ligand-directed dibromophenyl benzoate chemistry for rapid and selective acylation of intracellular natural proteins. *Chem. Sci.* **6**, 3217–3224 (2015).
17. Tamura, T. et al. Rapid labelling and covalent inhibition of intracellular native proteins using ligand-directed N-Acyl-N-Alkyl sulfonamide. *Nat. Commun.* **9**, 1–12 (2018).
18. Moss, S. M., Jayasekara, P. S., Paoletta, S., Gao, Z. G. & Jacobson, K. A. Structure-based design of reactive nucleosides for site-specific modification of the A2A adenosine receptor. *ACS Med. Chem. Lett.* **5**, 1043–1048 (2014).
19. Stoddart, L. A. et al. Ligand-directed covalent labelling of a GPCR with a fluorescent tag in live cells. *Commun. Biol.* **3**, 1–9 (2020).
20. Beerkens, B. L. H. et al. N-Acyl-N-Alkyl sulfonamide probes for ligand-directed covalent labeling of GPCRs: the adenosine A2B receptor as case study. *ACS Chem. Biol.* **19**, 1554–1562 (2024).
21. Arttamangkul, S. et al. Visualizing endogenous opioid receptors in living neurons using ligand-directed chemistry. *Elife* **8**, e49319 (2019).
22. Adoff, H., Halls, V. S., Holland, E., Lobingier, B. & Arttamangkul, S. Ligand-directed labeling of opioid receptors for covalent attachment of fluorophores or small-molecule probes. *STAR Protoc.* **4**, 102231 (2023).
23. Arttamangkul, S., Platt, E. J., Carroll, J. & Farrens, D. L. Functional independence of endogenous M- and δ-opioid receptors co-expressed in cholinergic interneurons. *Elife* **10**, e69740 (2021).
24. Kosar, M. et al. Platform reagents enable synthesis of ligand-directed covalent probes: study of cannabinoid receptor 2 in live cells. *J. Am. Chem. Soc.* **145**, 15094–15108 (2023).
25. Comeo, E. et al. Ligand-directed labeling of the adenosine A1 receptor in living cells. *J. Med. Chem.* **67**, 12099–12117 (2024).

26. Wang, H. et al. Chemical cell-surface receptor engineering using affinity-guided, multivalent organocatalysts. *J. Am. Chem. Soc.* **133**, 12220–12228 (2011).
27. Tamura, T. et al. Affinity-guided oxime chemistry for selective protein acylation in live tissue systems. *J. Am. Chem. Soc.* **139**, 14181–14191 (2017).
28. Madras, B. K. et al. Fluorescent and biotin probes for dopamine receptors: D1 and D2 receptor affinity and selectivity. *Mol. Pharmacol.* **37**, 833–9 (1990).
29. Matsuo, K. et al. One-step construction of caged carbonic anhydrase I using a ligand-directed acyl imidazole-based protein labeling method. *Chem. Sci.* **4**, 2573–2580 (2013).
30. Izquierdo-Serra, M. et al. Optical control of endogenous receptors and cellular excitability using targeted covalent photoswitches. *Nat. Commun.* **7**, 1–12 (2016).
31. Garrido-Charles, A. et al. Fast photoswitchable molecular prosthetics control neuronal activity in the cochlea. *J. Am. Chem. Soc.* **114**, 9229–9239 (2022).
32. Pándy-Szekeres, G. et al. GPCRdb in 2018: adding GPCR structure models and ligands. *Nucleic Acids Res.* **46**, D440–D446 (2018).
33. Kooistra, A. J. et al. GPCRdb in 2021: integrating GPCR sequence, structure and function. *Nucleic Acids Res.* **49**, D335–D343 (2021).
34. Bakthavachalam, V., Baidur, N., Madras, B. K. & Neumeyer, J. L. Fluorescent probes for dopamine receptors: synthesis and characterization of fluoresein and 7-nitrobenz-2-oxa-1,3-diazol-4-Yl conjugates of D-1 and D-2 receptor ligands. *J. Med. Chem.* **34**, 3235–3241 (1991).
35. Kennedy, D. C. et al. Cellular consequences of copper complexes used to catalyze bioorthogonal click reactions. *J. Am. Chem. Soc.* **133**, 17993–18001 (2011).
36. Reddi, R. N. et al. Site-specific labeling of endogenous proteins using CoLDR chemistry. *J. Am. Chem. Soc.* **143**, 20095–20108 (2021).
37. Ryman-Rasmussen, J. P., Nichols, D. E. & Mailman, R. B. Differential activation of adenylate cyclase and receptor internalization by novel dopamine D1 receptor agonists. *Mol. Pharmacol.* **68**, 1039–1048 (2005).
38. Kotowski, S. J., Hopf, F. W., Seif, T., Bonci, A. & von Zastrow, M. Endocytosis promotes rapid dopaminergic signaling. *Neuron* **71**, 278–290 (2011).
39. Levoye, A. et al. A broad G protein-coupled receptor internalization assay that combines SNAP-tag labeling, diffusion-enhanced resonance energy transfer, and a highly emissive terbium cryptate. *Front. Endocrinol. (Lausanne)*. **6**, 167 (2015).
40. Shipley, M. M.; Mangold, C. A.; Szpara, M. L. Differentiation of the SH-SY5Y human neuroblastoma cell line. *JoVE J. Vis. Exp.* **60**, 1058–1067 (2016).
41. Dommerholt, J. et al. Highly accelerated inverse electron-demand cycloaddition of electron-deficient azides with aliphatic cyclooctynes. *Nat. Commun.* **5**, 1–7 (2014).
42. Oliveira, B. L., Guo, Z. & Bernardes, G. J. L. Inverse electron demand diels-alder reactions in chemical biology. *Chem. Soc. Rev.* **46**, 4895–4950 (2017).
43. Sebastianutto, I. et al. D1-MGlu5 heteromers mediate noncanonical dopamine signaling in parkinson's disease. *J. Clin. Invest.* **130**, 1168–1184 (2020).
44. Namkung, Y. et al. Monitoring G protein-coupled receptor and β -arrestin trafficking in live cells using enhanced bystander BRET. *Nat. Commun.* **7**, 1–12 (2016).
45. Rives, M. L. et al. Crosstalk between GABAB and MGlu1a receptors reveals new insight into GPCR signal integration. *EMBO J.* **28**, 2195–2208 (2009).
46. Schiele, F., Ayaz, P. & Fernández-Montalván, A. A universal homogeneous assay for high-throughput determination of binding kinetics. *Anal. Biochem.* **468**, 42–49 (2015).
47. Schiele, F., Ayaz, P. & Fernández-Montalván, A. Erratum: Corrigendum to “A universal, homogenous assay for high throughput determination of binding kinetics”. *Anal. Biochem.* **514**, 1 (2016).

Acknowledgements

The project on which these results are based has received funding from Agence Nationale de la Recherche (ANR-17-CE11-0046), Ministerio de Ciencia e Innovación, Agencia Estatal de Investigación and ERDF - A way of making Europe (projects CTQ2017-89222-R, PCI2018-093047 and PID2020-120499RB-I00) by the Catalan government (2021 SGR 00508) the European Union's Horizon 2020 research and innovation programme under Marie Skłodowska-Curie grant agreement No. 801342 (TecniopringINDUSTRY, TECSPR19-1-0062) and the Government of Catalonia's Agency for Business Competitiveness (ACCIÓ). We thank the Dr. David Hamilton for proof-reading and language support, ARPEGE Pharmacology-Screening-Interactome platform facility (UMS Bio-campus, Montpellier, France) for the use of the plate readers, the MRI Montpellier Ressources Imagerie (UMS Bio-campus, Montpellier, France), member of the France-Biolmaging national infrastructure supported by the French National Research Agency (ANR-10-INBS-04), «Investments for the future», for images acquisition, Lourdes Muñoz and Carme Serra from SIMChem (IQAC CSIC) for analytical support and helpful discussions, L. Clusan for the generation of the Flag-SNAPtag-D₁ receptor, S. Soldevila, E. Bourrier, K. Belkacemi, J. Haubrich, S. Panarello, F. Malhaire, J. Kniazeff, C. Lavergne and X. Rovira for helpful discussions and technical support.

Author contributions

Conceptualisation X.G.-S., L.P., J.Z., J.-P.P., A.L.; Methodology X.G.-S., M.B., J.C., E.M., J.P., L.P.; Validation X.G.-S.; J.C.; E.M., T.R.; E.T., J.P., L.P.; Formal analysis X.G.-S.; E.M.; Investigation X.G.-S., M.B., C.M.-J., M.C., J.C., E.M.; Resources X.G.-S., J.C., E.M., L.L., E.T., J.P., L.P.; Data Curation X.G.-S., M.C., J.C., E.M.; Writing—Original Draft X.G.-S., L.P., J.-P.P.; A.L.; Writing—Review and Editing X.G.-S., J.Z., J.P., L.P., J.-P.P., A.L.; Visualisation X.G.-S., M.B., M.C., E.M.; Supervision X.G.-S.; J.C., E.M., J.P., L.L., L.P., J.Z., J.-P.P., A.L.; Project administration L.L., J.Z., J.-P.P., A.L.; Funding acquisition J.Z., J.-P.P., A.L.

Competing interests

T.R., E.T., and L.L. are employees of the private company Revvity, Codolet, France. J.-P.P. is the scientific director of Eidos, a common laboratory with Revvity. J.-P.P. is acting as consultant for Givaudan and Pharvaris. All other authors declare no competing interests.

Additional information

Supplementary information The online version contains supplementary material available at <https://doi.org/10.1038/s42004-025-01504-3>.

Correspondence and requests for materials should be addressed to Xavier Gómez-Santacana, Jean-Philippe Pin or Amadeu Llebaria.

Peer review information *Communications Chemistry* thanks the anonymous reviewers for their contribution to the peer review of this work.

Reprints and permissions information is available at <http://www.nature.com/reprints>

Publisher's note Springer Nature remains neutral with regard to jurisdictional claims in published maps and institutional affiliations.

Open Access This article is licensed under a Creative Commons Attribution-NonCommercial-NoDerivatives 4.0 International License, which permits any non-commercial use, sharing, distribution and reproduction in any medium or format, as long as you give appropriate credit to the original author(s) and the source, provide a link to the Creative Commons licence, and indicate if you modified the licensed material. You do not have permission under this licence to share adapted material derived from this article or parts of it. The images or other third party material in this article are included in the article's Creative Commons licence, unless indicated otherwise in a credit line to the material. If material is not included in the article's Creative Commons licence and your intended use is not permitted by statutory regulation or exceeds the permitted use, you will need to obtain permission directly from the copyright holder. To view a copy of this licence, visit <http://creativecommons.org/licenses/by-nc-nd/4.0/>.

© The Author(s) 2025